Stability and Bifurcation Analysis of Reservoir Sedimentation Management

Ray Huffaker*, Devin Rider and Rollin H. Hotchkiss

Food and Resource Economics Department, University of Florida, Gainesville, FL 32611-0240, USA

Undergraduate Major in Computer Science, College of Engineering and Architecture, Washington State University, Pullman, WA 99164, USA

Department of Civil and Environmental Engineering, Brigham Young University, Provo, UT 84602-4028, USA

Abstract: The alarming loss of water storage capacity to sedimentation in reservoirs worldwide is prompting a paradigm shift toward sustainable management. Previous research has investigated the physical capability of various technologies to control reservoir sediment, and formulated economic rules governing their optimal sustainable use. We ask the next relevant questions: Is sustainable reservoir management structurally stable for particular technologies, or do thresholds exist such that small perturbations in key management parameters abruptly unleash dynamics driving the reservoir toward extinction? What are the dynamic properties of reservoirs in transition? We uncover a saddle-node bifurcation for the particular case of a multi-purpose public reservoir manager who adopts the environmentally friendly 'hydrosuction-dredging' sediment removal technology. Beyond the bifurcation threshold, sustainable management abruptly gives way to eventual loss of storage capacity to sedimentation.

Keywords: Reservoir sedimentation removal, sustainable reservoir management, hydrosuction dredging, bifurcation analysis.

INTRODUCTION

Dams obstruct rivers to store water in adjacent reservoirs and to increase hydraulic head (the difference in surface elevation between the upstream reservoir and the downstream river). This produces essential social services including hydropower generation; agricultural, domestic, and industrial water supplies; flood control; improved river navigation; and recreational opportunities. Dams also unintentionally obstruct the flow of sediment through river systems. Sediment entrapped in reservoirs reduces water storage capacity and hydraulic head [1].

Reservoirs throughout the world suffer from sedimentation. Examples include estimated annual storage capacity losses of 2.3% in China [2], 0.5% in India [2], and 1% worldwide [3]. Specific examples are catalogued by Batuca and Jordaan [4]. These include the Cir-lurtsk Reservoir on the Sulak River (Russia) which was 95% sedimented in 7 years; the Gumati Reservoir on the Vakhs River (Georgia) which was 90% sedimented in 11 years; and the Zemo Afchar Reservoir at the confluence of the Kura and Aragi Rivers (Russia) which lost 44% of its initial storage capacity in the first 2 years, 32% in the next 8 years, and 3.5% up to 1967. Other examples include the Tarbela Dam on the Indus River—the most important facility of its kind in Pakistan—which lost 20% of its storage capacity after 23 years of operation [5]; and the Matilija Dam in California whose storage capacity decreased from 7,000 acre feet in 1947 to less than 500 acre feet by 2005 [6].

*Address correspondence to this author at the Food and Resource Economics Department, University of Florida, Gainesville, FL 32611-0240, USA; Tel: 352-392-1826x204; Fax: 352-846-0988; E-mail: rhuffaker@ufl.edu

The large environmental and economic costs of restoring reservoir storage capacity by constructing new projects is prompting a paradigm shift toward preserving current capacity by managing existing projects in a sustainable manner [5, 7]. Sustainable reservoir management requires control technologies to remove sediment at its average annual rate of inflow [8].

Sediment control technologies are broadly categorized along two lines: (1) whether they employ hydraulic or mechanical technologies [4]; and (2) whether they seek to minimize sediment loads entering the reservoir, minimize the deposition of sediment in reservoirs, or extract sediments accumulated in the reservoir [1, 2]. Strategies seeking to minimize incoming sediment include controlling erosion in the catchment area, employing 'check dams' to trap sediments upstream of the reservoir, and 'bypassing' high river flows with large sediment concentrations. Hydraulic technologies controlling the deposition of sediments in reservoirs include 'sluicing' (incoming sediment-laden flood waters are run through the dam before sediment can settle in the reservoir), and 'density current venting' (incoming sediment-laden flow is routed under the stored water and through the dam's bottom outlets). Hydraulic technologies removing accumulated sediment include 'flushing' (sediment is flushed from the reservoir through the dam's bottom outlets during a flood event), and 'siphoning' (sediment is transported over or through the dam in a flexible pipeline submerged in the reservoir). Mechanical technologies used to evacuate accumulated sediment include excavation and dredging.

The literature on reservoir sedimentation management has evolved along two branches. The first branch is defined by numerous engineering studies formulating the physical

1874-3781/10

capacity of sediment control technologies. This work is summarized in several books [1, 2, 4]. The second branch is defined by a relatively few economic studies investigating the economic optimality of sustainable reservoir management.

Palmieri *et al*. [5] studied the economic dynamics of the sluicing sediment-routing technology. Sluicing releases a portion of annual water inflow (that might otherwise refill the reservoir for future consumption) to drive suspended sediment beyond the reservoir before it settles. They captured the essence of sluicing dynamics with a continuous-time single-state (water storage capacity) reservoir model. They embedded this into an optimal control formulation to determine the optimal volume of sediment to remove annually, and demonstrated the optimality of sustainable reservoir management for parameters characterizing a representative reservoir. The World Bank adopted this single-state specification to design a practical decision tool (RESCON) for selecting the optimal sediment control technology from alternatives including flushing, hydrosuction dredging, traditional dredging, trucking and no removal [9, 10].

Huffaker and Hotchkiss [11] investigated the economic dynamics associated with the newly emerging 'hydrosuction-dredging' (*HD*) siphoning technology [12]. *HD* employs the potential energy stored by the hydraulic head at the dam to draw sediment-entrained water into a submerged removal pipeline for transport downstream (Fig. **1**). The removal pipe—which goes through the dam—extends from the sedimented reservoir bottom to a discharge point downstream. *HD* is engineered to be environmentally friendly. It does not require diesel power pumps to transport sediment, thereby conserving fossil fuels and preventing oil spills in drinking-water reservoirs. Since *HD* relies on a chain of multidimensional hydraulic linkages suppressed in previous single-state modeling, Huffaker and Hotchkiss [11] formulated an interdependent two-state system including both reservoir water storage capacity and the volume of impounded water. They embedded these reservoir dynamics into a continuous-time optimal control formulation to determine the optimal volume of water to consume in non-hydrosuction uses (e.g., hydropower production and irrigation). Similar to Palmieri *et al*. [5], their results showed sustainable reservoir management to be optimal for representative parameters.

To our knowledge, past work has not investigated the threat to sustainable reservoir management posed by 'bifurcation thresholds' resulting from small perturbations in key sediment management parameters in the neighborhood of equilibria. On one side of such thresholds, sustainable resource management is a feasible option for at least some range of initial reservoir storage capacities. Once such thresholds are crossed, sustainable management is no longer a feasible option for any initial capacities. The only feasible option is for the reservoir to eventually become chocked off by sediment. It is time to ask two further questions: Do bifurcation thresholds exist for sediment control technologies recommended in the literature? What are the dynamic properties of reservoirs in transition?

METHODS

We posit the following realistic reservoir management scenario: A manager has contractual obligations to provide impounded water for consumptive activities including hydropower production, irrigation, municipal/industrial water supplies, and so on. The manager is authorized to modify contractual obligations to protect public interests, including the long-term storage capacity of the dam/reservoir project. Reservoirs under this general type of management system include multi-purpose public projects. For example, the U.S. Army Corps of Engineers is authorized by federal statute (33 U.S.C. § 403) to grant permits contracting irrigation of a fixed number of acres with water pumped from approved reservoirs. The Corps retains the authority to modify permits "if it is determined that, under existing circumstances, modification is in the public interest" [13]. We focus on the particular case in which stored water is required to protect water storage capacity by removing impounded sediment through the *HD* pipeline.

Following past analytical studies [5, 11], we formulate a continuous-time model of reservoir management. We ap-

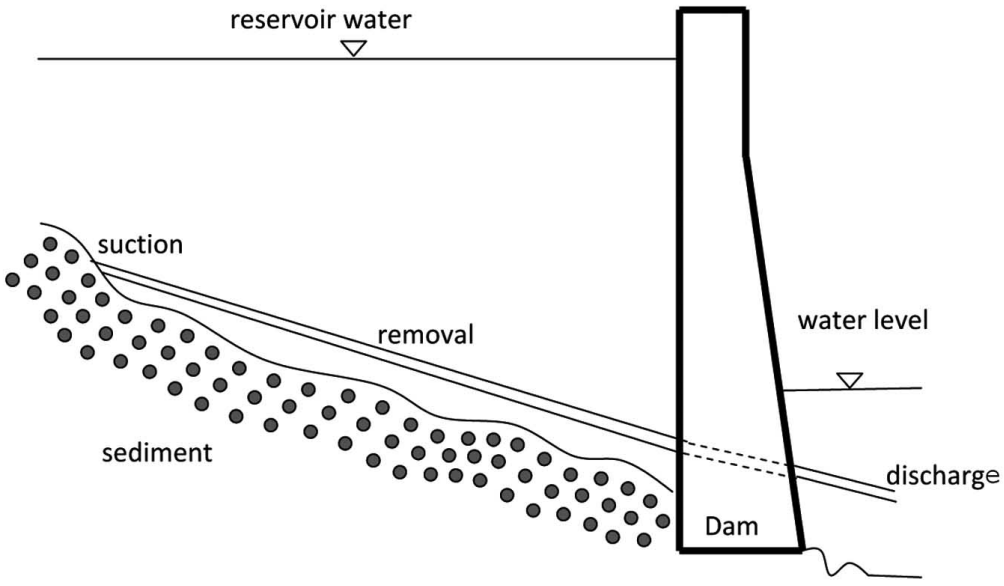

Fig. (1). Hydrosuction-dredging sediment removal technology.

proximate real-world management by formulating a feedback policy that reduces contractual obligations when impounded water is required for a public purpose; in this case, to provide potential energy for *HD* sediment removal. In particular, management sets a maximum allowable consumption rate (C^m) of impounded water to meet contractual obligations when the reservoir is at full water storage capacity. As storage capacity is lost to sedimentation, the policy promotes sustainable reservoir use by decreasing the C^m rate proportionately to remaining capacity. This recovers storage capacity by increasing the volume of impounded water providing potential energy for *HD* sediment transport.

We next conduct a bifurcation analysis to study the structural stability of reservoir equilibria for small perturbations in the C^m rate with other parameters held constant. The analysis uncovers a 'saddle-node' bifurcation: C^m rates below the bifurcation threshold produce two branches of equilibria consistent with sustainable reservoir management from a range of initial storage capacities. The equilibria disappear for C^m rates above the threshold, and the reservoir evolves toward 'extinction' for all initial storage capacities.

We draw hydrologic parameter values required to solve our model from a case study of the Tianjiawan reservoir on the Jian River in Yuci, Shanzi province, China [14]. The reservoir was built in 1960 with a storage capacity of 9.425 million m^3, and an annual sediment load of 0.25 million m^3. In the first 15 years, the reservoir accumulated about 4.0 million m^3 of deposited sediment. Since 1975, a siphon sediment removal system has been used consisting of a submerged floating pipeline—of 229*m* in length and 550*mm* in diameter—connected to the dam outlet.

Dimensional Reservoir Model

The interdependent dynamics of impounded reservoir water $\left(W_t, m^3\right)$ and remaining reservoir storage capacity $\left(S_t, m^3\right)$ follow along the lines of [11]:

$$\frac{dW}{dt} = \underbrace{R\left(W_t, S_t\right)}_{\text{refill}} - \underbrace{C\left(W_t, S_t; C^m\right)}_{\text{contractual obligations}} - \underbrace{HD_W\left(W_t, S_t\right)}_{\substack{\text{sediment-entrained water} \\ \text{drawn through } HD \text{ pipeline}}} - \underbrace{EV\left(W_t\right)}_{\text{evaporation}} \tag{1a}$$

$$\frac{dS}{dt} = \underbrace{HD_{SD}\left(W_t, S_t\right)}_{\text{sediment transport rate}} - \underbrace{SI}_{\substack{\text{sediment} \\ \text{entrapment rate}}} \tag{1b}$$

The volume of impounded water changes at a net annual rate $\left(m^3/t\right)$ in (1a) equaling the difference between the annual refill rate and the rates at which impounded water is consumed in three major activities: meeting contractual obligations, *HD* sediment transport, and evaporative losses. Remaining reservoir storage capacity changes at a net annual rate $\left(m^3/t\right)$ in (1b) equaling the difference between the rate at which sediment is transported by *HD* and a fixed annual rate at which sediment is entrapped in the reservoir. The functional forms characterizing the rates in (1a, b) are discussed below. The associated variables and parameters are summarized in Table **1**.

The reservoir accommodates additional water each year proportionate to the difference between remaining storage capacity and water already impounded: $R\left(W_t, S_t\right) = \alpha_1\left(S_t - W_t\right)$, where α_1 $\left(1/t\right)$ is fixed at unity. Additional water exceeding remaining storage capacity is involuntarily spilled.

The annual consumption rate of impounded water available to meet contractual obligations is modeled with a Michaelis-Menton function (graphed in Fig. **2**):

$$C\left(W_t, S_t; C^m\right) = \Gamma_1 W_t / \left(W_t + \Gamma_2\right) \tag{2a}$$

$$\Gamma_1 = C^m\left(S_t / S^m\right) \tag{2b}$$

$$\Gamma_2 = \alpha_2\left[1 - \left(S_t / S^m\right)\right] \tag{2c}$$

The annual consumption rate function (2a) depends on two composite parameters: Γ_1 and Γ_2. Mathematically speaking, Γ_1 gives the horizontal asymptote of $C\left(W_t, S_t; C^m\right)$ as stored water increases toward infinity, and Γ_2 is the stored water level yielding half of this asymptote, 0.5 Γ_1. Composite parameter Γ_2 is inversely related to the annual consumption rate of impounded water, $C\left(W_t, S_t; C^m\right)$, indicating that smaller values of Γ_2 cause $C\left(W_t, S_t; C^m\right)$ to adjust more rapidly toward its maximum rate Γ_1.

The behavior of composite parameter Γ_1 is given by (2b). When the reservoir is at maximum storage capacity, S_t = S^m $\left(m^3\right)$, Γ_1 equals the 'maximum allowable consumption' rate C^m $\left(m^3/t\right)$, and $C\left(W_t, S_t; C^m\right)$ asymptotically increases from zero (when the stock of impounded water is zero) toward C^m (as impounded water increases). As storage capacity is lost ($S_t < S^m$), C^m adjusts downward proportionately to the fraction of remaining storage capacity: $C^m\left(S_t / S^m\right)$.

The behavior of composite parameter Γ_2 is given by (2c). When the reservoir is at full storage capacity, $S_t = S^m$, $C\left(W_t, S_t; C^m\right)$ adjusts instantaneously to the C^m rate. Alternatively, as the reservoir becomes sedimented, $C\left(W_t, S_t; C^m\right)$ adjusts more slowly to the C^m rate. This increases future storage capacity by increasing the volume of water left impounded (unconsumed) to provide potential energy for *HD* sediment transport.

To model *HD* sediment transport, we first specify an elevation-storage curve because the reservoir's surface elevation

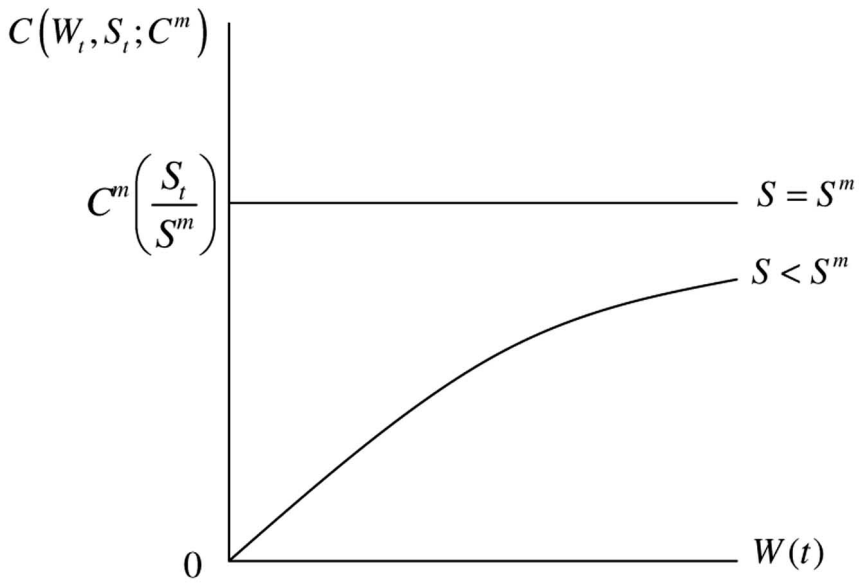

Fig. (2). The annual consumption rate of impounded water to meet contractual obligations.

provides the potential energy for the process. Empirical elevation-storage curves show that surface elevation increases at a decreasing rate with the volume of impounded water [1, 15]. Consequently, we employ a Michaelis-Menton function which increases elevation asymptotically toward E^m (m)—the maximum elevation to which the reservoir surface can rise during ordinary operating conditions ('normal pool level')—as impounded water increases.

$$E\left(W_t, S_t\right) = E^m W_t / \left[W_t + \left(\alpha_5 + \alpha_6 S_t\right)\right] \tag{3}$$

The term $\left(\alpha_5 + \alpha_6 S_t\right)$ measures the volume of impounded water for which surface elevation reaches half of it maximum level (0.5 E^m), and consequently is inversely related to the efficiency with which impounded water is converted to maximum surface elevation. Consistent with empirical elevation-storage curves, this term is designed to shift $E\left(W_t, S_t\right)$ to the left as remaining storage capacity decreases due to sedimentation. This has the impact of increasing the elevation obtained by each volume of impounded water. The justification is that impounded water becomes 'perched' upon an enlarged layer of sediment. Ironically, sediment perching increases the potential energy for *HD* transport by increasing reservoir surface elevation—a 'bad' does some 'good'.

The annual rate at which sediment is transported by the *HD* pipeline is roughly proportional to surface elevation for typical parameters (i.e., pipeline length, diameter, and material) and intermediate-sized reservoirs [11]: $HD_{SD}\left(W_t, S_t\right) = \alpha_4 E\left(W_t, S_t\right)$,

where α_4 $\left(m^3 t^{-1} / m\right)$ is the proportionality parameter.

Following Kawashima *et al.* [10], we assume that the annual rate at which water is required to drawn sediment through the *HD* pipeline is proportional to the sediment transport rate by parameter α_3 (unitless): $HD_W\left(W_t, S_t\right) = \alpha_3 HD_{SD}\left(W_t, S_t\right)$.

Evaporative losses sustained by reservoirs in hot and arid climates are typically approximated as a proportion of a reservoir's average water surface area [16]. Since these losses are not the focal point of our model, we account for them more simply as a constant proportion α_7 $\left(1/t\right)$ of impounded water: $EV\left(W_t\right) = \alpha_7 W_t$.

Finally, sediment is assumed to be entrapped in the reservoir at a fixed annual rate: $SI = \alpha_8$ $\left(m^3 / t\right)$.

Dimensionless Reservoir Model

The number of system parameters can be reduced from ten to six by scaling the dimensional system (1) to the following dimensionless variables: $s_t = S_t / S^m$ (fraction of maximum storage capacity remaining), $w_t = W_t / S^m$ (fraction of maximum storage capacity of impounded water), and $\tau = \alpha_1 t$ (dimensionless time variable):

$$\frac{dw}{d\tau} = \dot{w} = s_t - w_t - \left\{c^m s_t w_t / \left[w_t + \beta_1\left(1 - s_t\right)\right]\right\} - \alpha_3\left[\beta_2 w_t / \left(w_t + \beta_3 + \alpha_6 s_t\right)\right] - \beta_4 w_t \tag{4a}$$

$$\frac{ds}{d\tau} = \dot{s} = \left[\beta_2 w_t / \left(w_t + \beta_3 + \alpha_6 s_t\right)\right] - \beta_5 \tag{4b}$$

where $c^m = C^m / \left(\alpha_1 S^m\right)$ is a dimensionless parameter measuring the maximum allowable consumption rate as a fraction of maximum reservoir storage capacity. The definitions and interpretations of the other dimensionless parameters are reported in Table **1** $\left(\alpha_1, \alpha_3, \alpha_6\right)$ and Table **2** $\left(\beta_1 \text{ through } \beta_5\right)$.

Table 1. Dimensional Variables and Parameters

Variables	Description	Units	
S_t	remaining storage capacity	m^3	
W_t	volume of impounded water	m^3	
t	time	Years	
Parameters			Values
S^m	maximum storage capacity	m^3	9,430,000 [a]
α_1	refill rate parameter	t^{-1}	1
C^m	maximum allowable consumption rate of impounded water to satisfy contractual obligations	m^3t^{-1}	3,772,000 [c]
$\alpha_2\left(1-\frac{S_t}{S^m}\right)$	volume of impounded water giving half of maximum allowable consumption rate	m^3	α_2 = 3,000,000 [c]
α_3	proportion of water needed to remove a unit of sediment	--	6.41[b]
α_4	slope of sediment transport-elevation function	m^3t^{-1} /meter	47,000[b]
E^{max}	maximum reservoir elevation	Meters	17.4[a]
α_5 (α_6)	slope (intercept) of elevation-storage water efficiency	m^3 (--)	1 (1)[c]
α_7	proportional evaporation rate	t^{-1}	0.02[c]
α_8	annual sediment entrapment rate	m^3t^{-1}	250,000[a]

[a]These parameter values are drawn directly from Liu *et al*. [14]. We assume that the maximum reservoir elevation $\left(E^{\max}\right)$ is the 'gross' head (vertical distance in surface elevation between the upstream reservoir and downstream river) reported in Liu *et al.* [14].

[b]These parameter values are calculated from data in Liu *et al*. [14]. We calculate α_3 as the inverse of the reported sediment-water ratio of 15.6%. We calculate α_4 as the ratio of dredged sediment (320,000 m^3) to 'effective' head (6.81 m). Effective head is the gross head corrected for water losses through trashracks, valves, penstocks, etc. In sum, effective head is the elevation providing potential energy for *HD* transport. Lui *et al*. [14] report that effective head for Tianjiawan Reservoir is in the interval of 5.5 to 8.8 *m*.

[c]These parameter values are unavailable from Liu *et al*. [14]. Values are selected that generate reasonable results in numerical simulations in combination with known values. For example, the maximum allowable consumption rate of impounded water to satisfy contractual obligations, C^m, is set at 40% of the reservoir's maximum storage capacity, S^m.

Table 2. Dimensionless Variables and Parameters

Variables	Definition
$s_t = \frac{S_t}{S^m}$	fraction of maximum storage capacity remaining
$w_t = \frac{W_t}{S^m}$	fraction of maximum storage capacity of impounded water
$\tau = \alpha_1 t$	time variable
Parameters	
$c^m = \frac{C^m}{\alpha_1 S^m}$	fraction of maximum storage capacity of maximum consumption rate of storage water in non-hydrosuction activities
$\beta_1 = \frac{\alpha_2}{S^m}$	consumption function rate of adjustment parameter
$\beta_2 = \frac{\alpha_4 E^m}{\alpha_1 S^m}$	sediment transport function parameter
$\beta_3 = \frac{\alpha_5}{S^m}$	sediment transport function parameter
$\beta_4 = \frac{\alpha_7}{\alpha_1}$	proportional evaporation rate
$\beta_5 = \frac{\alpha_8}{\alpha_1 S^m}$	fraction of maximum storage capacity of sediment entrapment rate

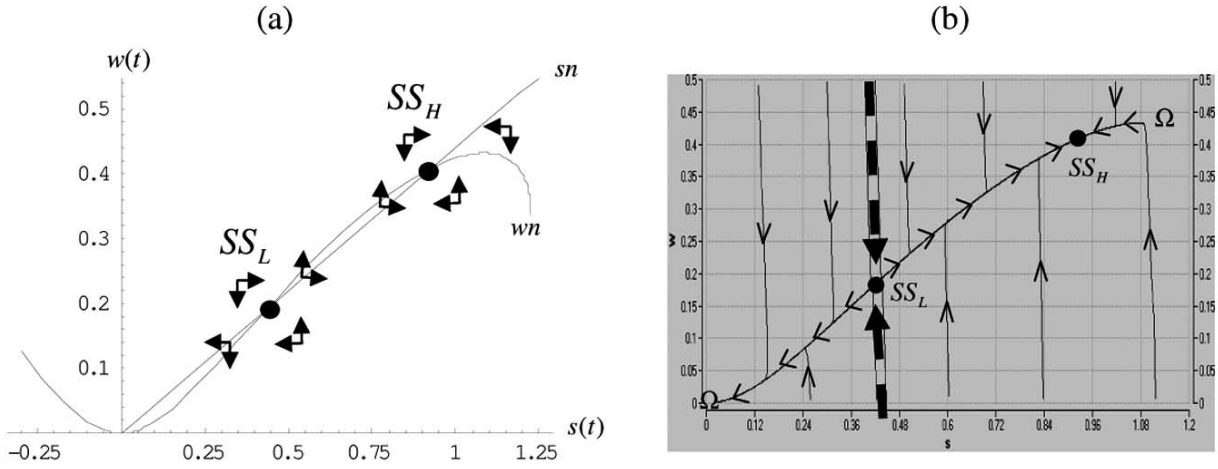

Fig. (3). Phase diagram of system (4) for baseline parameters: (**a**) graphs of nullclines and directions of motion (*Mathematica*); (**b**) numerically generated phase diagram (*Berkeley Madonna* software).

Solution of Dimensionless Model

We solve system (4) numerically with baseline parameters values drawn from a case study of *HD* sediment transport in the Tianjiawan reservoir, China [14], and reported in Table **1**. To illustrate system dynamics exhibiting sustainable reservoir use, we arbitrarily set the maximum allowable consumption rate of impounded water at 40% of maximum storage capacity: $C^m = 0.4S^m = 3{,}772{,}000 \quad m^3t^{-1}$. The corresponding dimensionless value is: $c^m = C^m / \left(\alpha_1 S^m\right) = 0.4$.

The nullclines associated with (4) are shown in Fig. **3**(**a**). Nullcline *wn* is the curvilinear graph of impounded-water (*w*) and storage-capacity (*s*) combinations that set $\dot{w} = 0$ in (4a) by balancing the reservoir-refill rate with the rates at which reservoir water is consumptively used in satisfying contractual obligations, *HD* sediment transport, and evaporation. Nullcline *sn* is the linear curve of impounded-water and storage-capacity combinations that set $\dot{s} = 0$ in (4b) by balancing sediment inflow and removal rates. Storage capacity increases (decreases) over time for impounded water volumes above (below) *sn* because the potential energy supplied by the reservoir allows (does not allow) the *HD* pipeline to remove sediment at a greater rate than it enters.

The nullclines intersect at two equilibria: SS_L $\left(s_L^{ss} = 0.427, w_L^{ss} = 0.188\right)$ and SS_H $\left(s_H^{ss} = 0.935, w_H^{ss} = 0.412\right)$. SS_L is characterized by volumes of impounded water and storage capacity that are relatively lower than those characterizing SS_H. Linear stability analysis produces real eigenvalues of opposite sign in the neighborhood of SS_L $\left(-1.917, 0.012\right)$, and negative real eigenvalues in the neighborhood of SS_H $\left(-1.38, -0.0083\right)$. Thus, SS_L is a saddle point* and SS_H is a stable node† (Fig. **3**(**a**). Since both equilibria are hyperbolic (i.e., the eigenvalues of the linear flow at equilibrium all have nonzero real parts), the Stable Manifold Theorem guarantees that linear stability properties hold for the nonlinear flow, and are robust for small perturbations of (4) [17].

Solution trajectories for the baseline parameter values are shown in Fig. **3**(**b**). Impounded water volumes converge rapidly along vertical trajectories toward a solution manifold (denoted as Ω) comprised of the divergent separatrices associated with saddle point SS_L, and convergent trajectories associated with stable node SS_H. In particular, the divergent separatrix to the right of SS_L is a heteroclinic orbit linking SS_L with SS_H. Upon reaching Ω, impounded-water and storage-capacity volumes evolve relatively slowly along the manifold.

The dynamics along Ω are characterized by two basins of attraction separated by the convergent separatrices associated with lower-volume equilibrium SS_L (thickened dashed trajectories for emphasis). Storage capacities to the left of this boundary evolve along Ω toward the origin. The reservoir eventually fills up with sediment and loses its capacity to impound water. The reductions in storage capacity and impounded water along this section of Ω have offsetting impacts on the reservoir surface elevation that provides potential energy for *HD* sediment removal (3). The loss of storage capacity increases surface elevation due to sediment perching, but the reduction in impounded water reduces elevation for a given storage capacity. For the baseline parameters, the net effect is that surface elevation decreases along with the potential energy for *HD* transport. The reservoir is managed as a non-sustainable asset.

Alternatively, relatively larger storage capacities to the right of this boundary gravitate along Ω toward the higher-volume equilibrium, SS_H. Impounded water increases over time with expanded storage capacity. The potential energy for *HD* transport increases because the positive impact of increased volumes of impounded water on reservoir surface elevation out-weights the negative impact of reduced sedi-

* A saddle point equilibrium is characterized by a 'stable arm' solution trajectory parallel to which other trajectories approach equilibrium before eventually veering away; and an 'unstable arm' solution trajectory parallel to which other trajectories asymptotically veer away from equilibrium.

† A stable node equilibrium is characterized by solution trajectories that asymptotically approach equilibrium from all initial values of the state variables.

ment perching as storage capacity expands. The *HD* pipeline is able to remove sediment at a greater rate than it enters the reservoir. The reservoir is managed as a sustainable asset.

We proceed to search for a bifurcation-threshold of the maximum-allowable impounded-water consumption rate $\left(c^m\right)$ beyond which the possibility of sustainable reservoir management is foreclosed.

Bifurcation Analysis

Bifurcation points occur only at a 'non-hyperbolic' equilibrium, SS_{nh}, for which at least one of the eigenvalues of the linear flow at equilibrium has a zero real part [17]. Consequently, the criterion for detecting a bifurcation point for system (4) is to find values of c^m resulting in zero-valued or purely-imaginary eigenvalues. Fig. (**4**) plots numerical calculations of one of the two eigenvalues associated with the upper and lower steady states (SS_L with SS_H) for increasing levels of c^m (other baseline parameters held constant). A zero eigenvalue $\left(\lambda_1 = 0\right)$ occurs for $c^m_{nh} = 0.483$ (i.e., when the scaled maximum allowable impounded-water consumption rate reaches 48.3% of maximum storage capacity). The second calculated eigenvalue is $\lambda_2 = -1.781$. The associated non-hyperbolic equilibrium is $SS_{nh} = \left(\underbrace{0.586}_{s^{SS}_{nh}}, \underbrace{0.258}_{w^{SS}_{nh}}\right)$.

In contrast to hyperbolic equilibria, the Stable Manifold Theorem cannot be invoked to guarantee that SS_{nh} is structurally stable, or that linear stability properties hold for the nonlinear flow. Radically new dynamic behavior can occur for small shifts in parameters. Instead, the stability properties of SS_{nh} are governed by the Center Manifold Theorem [17]. The zero eigenvalue gives rise to a center manifold in phase space, and stability properties are resolved by studying the dynamics of system (4) restricted to this manifold in the neighborhood of SS_{nh}.

Computing the center manifold requires that system (4) be converted to the following generalized 'normal' form for the case of one zero $\left(\lambda_1 = 0\right)$, and one negative $\left(\lambda_2 < 0\right)$ eigenvalue [18]:

$$\begin{bmatrix} \frac{dx}{dt} \\ \frac{dy}{dt} \end{bmatrix} = \begin{bmatrix} \lambda_1 = 0 & 0 \\ 0 & \lambda_2 < 0 \end{bmatrix} \begin{bmatrix} x(t) \\ y(t) \end{bmatrix} + \begin{bmatrix} f(x(t), y(t), \varepsilon) \\ g(x(t), y(t), \varepsilon) \end{bmatrix} \qquad (5)$$

$$\frac{d\varepsilon}{dt} = 0$$

where $\left(x, y, \varepsilon\right) = \left(0,0,0\right)$ is the nonhyperbolic equilibrium of (5), and ε is a perturbation parameter treated as an additional dependent variable with no dynamics. Nonlinear functions $f\left(x(t), y(t), \varepsilon\right)$ and $g\left(x(t), y(t), \varepsilon\right)$ are restricted as follows: (1) $f(0,0,0) = 0 = g(0,0,0)$; and (2) $Df(0,0,0) = 0 = Dg(0,0,0)$, where D is the Jacobian operator.

The normal form for system (4) is:

$$\begin{pmatrix} \dot{w}_2 \\ \dot{s}_2 \end{pmatrix} =$$

$$\begin{pmatrix} -1.781 & 0 \\ 0 & 0 \end{pmatrix} \begin{pmatrix} w_2 \\ s_2 \end{pmatrix} + \begin{pmatrix} \underbrace{0.452109 s_2^2 - 1.02656 c_m^1 s_2 + 0.311589 c_1^m - 1.13003 w_2^2 - 0.886238 s_2 w_2 - 0.518379 c_1^m w_2}_{f\left(s_2, w_2, c_1^m\right)} \\ \underbrace{0.02011962 s_2^2 - 0.0456814 c_m^1 s_2 + 0.0138656 c_1^m + 0.0396664 w_2^2 + 0.0842781 s_2 w_2 - 0.0230677 c_1^m w_2}_{g\left(s_2, w_2, c_1^m\right)} \end{pmatrix} \qquad (6a)$$

$$\dot{c}_1^m = 0 \qquad (6b)$$

where $\dot{w}_2 = \frac{dw_2}{d\tau}$, $\dot{s}_2 = \frac{ds_2}{d\tau}$, and w_2 and s_2 are transformed impounded water and storage capacity variables, respectively. The derivation of normal form (6) is given in the Appendix.

The center manifold associated with normal form (6) is represented in the neighborhood of equilibrium $\left(s_2, w_2, c_1^m\right) = \left(0,0,0\right)$ as:

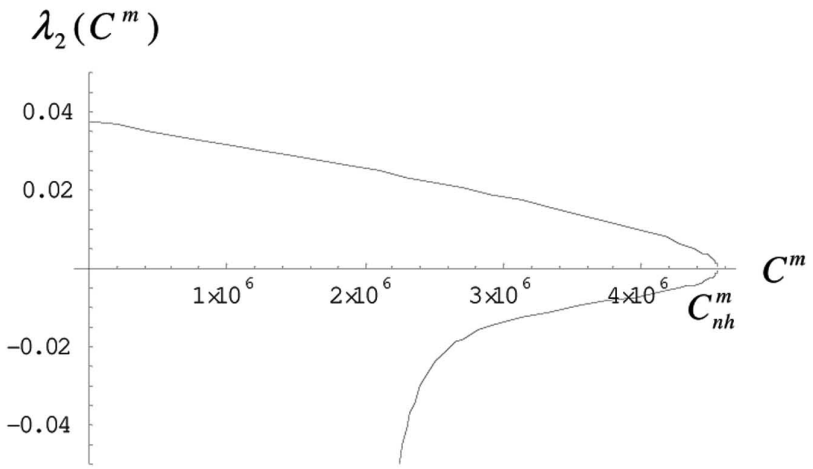

Fig. (4). Graph of one of the two eigenvalues associated with the upper and lower steady states for increasing levels of c^m (*Mathematica*).

$$W^c(0)=\left\{\left(s_2,w_2,c_1^m\right)\middle| w_2=h_c\left(s_2,c_1^m\right),h_c(0,0)=0,Dh_c(0,0)=0\right\} \quad (7)$$

In words, the $\left(s_2,w_2,c_1^m\right)$ coordinates on $W^c(0)$ must satisfy the center manifold equation:

$$w_2=h_c\left(s_2,c_1^m\right) \quad (8)$$

Variable s_2 serves as the dependent variable since the zero eigenvalue is found in the $\dot{s}_2$ equation (6a) [18]. The conditions $h_c(0,0)=0=Dh_c(0,0)$ ensure that the local representation of the center manifold is tangent to the corresponding generalized eigenspace associated with the zero eigenvalue at equilibrium [17].

In addition, the coordinates on $W^c(0)$ must satisfy the time derivative of the center manifold equation:

$$\dot{w}_2=\frac{\partial h_c}{\partial s_2}\dot{s}_2+\frac{\partial h_c}{\partial c_1^m}\dot{c}_1^m=\frac{\partial h_c}{\partial s_2}\dot{s}_2 \quad (9)$$

where $\dot{c}_1^m=0$ by (6b). Substituting $\dot{w}_2$ and $\dot{s}_2$ from (6a), along with the center manifold equation (8), into (9) yields:

$$\underbrace{-1.78\underbrace{h_c\left(s_2,c_1^m\right)}_{w_2}+f\left(s_2,\underbrace{h_c\left(s_2,c_1^m\right)}_{w_2},c_1^m\right)}_{\frac{dw_2}{d\tau}}=\underbrace{\frac{\partial h_c}{\partial s_2}g\left(s_2,\underbrace{h_c\left(s_2,c_1^m\right)}_{w_2},c_1^m\right)}_{\frac{ds_2}{d\tau}} \quad (10)$$

or equivalently:

$$N\left(h_c\left(s_2,c_1^m\right)\right)\equiv\frac{\partial h_c}{\partial s_2}g\left(s_2,h_c\left(s_2,c_1^m\right),c_1^m\right)+1.78h_c\left(s_2,c_1^m\right)-f\left(s_2,h_c\left(s_2,c_1^m\right),c_1^m\right)=0 \quad (11)$$

where functions $f\left(s_2,w_2,c_1^m\right)$ and $g\left(s_2,w_2,c_1^m\right)$ are defined in (6a). Equation (11) is a partial differential equation that is solved for the center manifold equation, $w_2=h_c\left(s_2,c_1^m\right)$.

An approximation theorem allows $h_c\left(s_2,c_1^m\right)$ to be computed to any desired degree of accuracy by solving (11) to the same degree of accuracy [18]. Consequently, we can pose the following power series expansion for $h_c\left(s_2,c_1^m\right)$:

$$w_2=h_c\left(s_2,c_1^m\right)=a_1s_2^2+a_2s_2c_1^m+a_3\left(c_1^m\right)^2+\ldots \quad (12)$$

where a_1, a_2, and a_3 are unknown constants. Substituting (12) into (11), and retaining only terms of the same order as (12), yields:

$$N\left(s_2,c_1^m\right)=0=0.0138656a_2\left(c_1^m\right)^2+1.78086a_3\left(c_1^m\right)^2+1.02656c_1^ms_2+0.0277312a_1c_1^ms_2+1.78086a_2c_1^ms_2-0.452109s_2^2+1.78086a_1s_2^2+\ldots \quad (13)$$

We solve (13) for a_1, a_2, and a_3 by equating coefficients:

s_2^2 term: $-0.452109+1.78086a_1=0 \Rightarrow a_1=0.253871$

$c_1^ms_2$ term: $1.02656+0.0277312a_1+1.780869a_2=0$

$\Rightarrow a_2=-0.580394$

$\left(c_1^m\right)^2$ term: $0.0138656a_2+1.78086a_3=0 \Rightarrow a_3=0.00451889$

Substituting these coefficients into (12) gives the numerical center manifold equation:

$$w_2=h\left(s_2,c_1^m\right)=0.253871s_2^2-0.580394s_2c_1^m+0.00451889\left(c_1^m\right)^2+\ldots \quad (14)$$

The dynamics of normalized system (6) reduced to the center manifold are obtained by substituting center manifold equation (14) into $\dot{s}_2$ in (6a):

$$\dot{s}_2=0.0201196s_2^2-0.0456814c_m^1s_2+0.0138656c_1^m+\ldots \quad (15)$$

RESULTS

The dynamics of (15) satisfy the general conditions for a saddle-node bifurcation in the neighborhood of equilibrium, $\left(s_2,w_2,c_1^m\right)=(0,0,0)$:

$$\dot{s}_2\left(\underbrace{0}_{s_2},\underbrace{0}_{c_1^m}\right)=0.0201196\left(\underbrace{0}_{s_2^2}\right)-0.0456814\left(\underbrace{0}_{c_1^m}\right)\left(\underbrace{0}_{s_2}\right)+0.0138656\left(\underbrace{0}_{c_1^m}\right)=0 \quad (16a)$$

$$\frac{\partial\dot{s}_2}{\partial s_2}(0,0)=2(0.0201196)\left(\underbrace{0}_{s_2}\right)-0.0456814\left(\underbrace{0}_{c_1^m}\right)=0 \quad (16b)$$

$$\frac{\partial\dot{s}_2}{\partial c_1^m}(0,0)=-0.0456814\left(\underbrace{0}_{s_2}\right)+0.0138656\neq 0 \quad (16c)$$

$$\frac{\partial\dot{s}_2}{\partial s_2^2}(0,0)=2(0.0201196)\neq 0 \quad (16d)$$

where (16a,b) are the conditions defining a nonhyperbolic equilibrium [18].

The bifurcation diagram plotting equilibria of (15), s_2^{SS}, against the bifurcation parameter, c_1^m, is shown in Fig. (**5**). For $c_1^m<0$ (indicating that the maximum-allowable impounded-water consumption rate c^m is less than the bifurcation rate c_{nh}^m equaling 48.3% of maximum reservoir storage capacity), there are two branches of storage capacity equilibria:

$$s_2^{SSu}=0.0456814c_1^m+24.8514\sqrt{-0.00117558c_1^m+0.00208679c_1^{m2}}$$

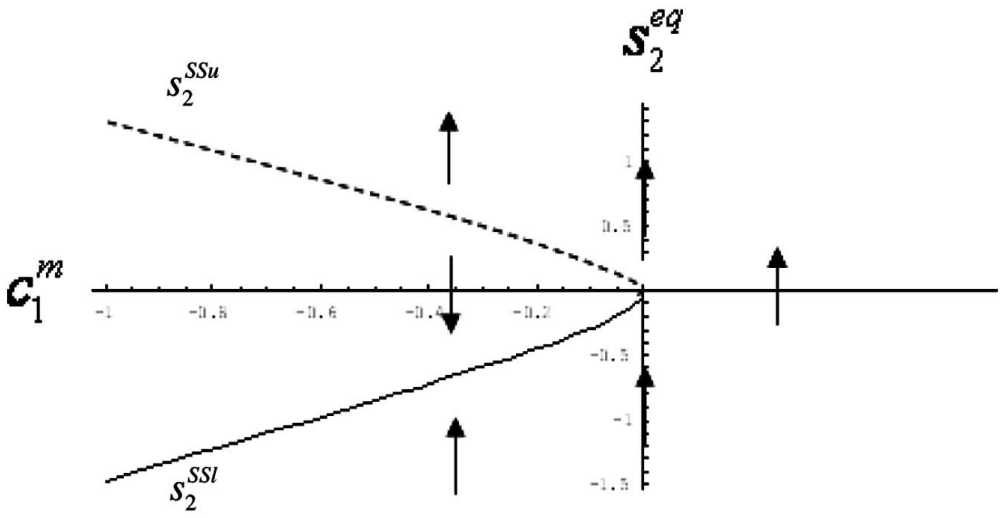

Fig. (5). Bifurcation diagram plotting equilibria of (17) against c_1^m (*Mathematica*).

$$s_2^{SSl} = 0.0456814c_1^m - 24.8514 \sqrt{-0.00117558c_1^m + 0.00208679c_1^{m2}}$$

Linear stability analysis shows that the upper branch, s_2^{SSu} (dashed line), is always unstable, while the lower branch, s_2^{SSl}, is stable for the baseline parameters. For $c_1^m > 0$ (indicating that c^m is greater than the bifurcation rate, $c_{nh}^m = 0.483$), (15) has no equilibria.

These results demonstrate that reservoir dynamics abruptly change for the worse in this case study when the maximum allowable consumption rate exceeds the 48.3% threshold of maximum reservoir storage capacity for the baseline parameters. Both equilibria are destroyed—along with the potential for sustainable reservoir management—because the volumes of impounded water and storage capacity required to balance impounded water dynamics (4a) are insufficient to balance sedimentation dynamics (4b) (i.e., the *wn* nullcline lies below the *sn* nullcline for all storage capacities in Fig. **3**(**a**)). Due to contractual obligations that are overly large in proportion to maximum storage capacity, the reservoir can not furnish the volume of impounded water providing the potential energy required for the *HD* pipeline to remove sediment at its inflow rate.

Larger bifurcation thresholds, c_{nh}^m, permit sustainable reservoir use over a broader range of maximum allowable consumption rates of impounded water. Thresholds can be shown numerically to increase in response to larger maximum storage capacities (Fig. **6a**), reduced sediment entrapment rates (Fig. **6b**), and reduced proportions of water required to transport a unit of sediment through the *HD* pipeline (Fig. **6c**). The first two measures (Figs. **6a**, **b**) reflect the conventional practice of prolonging the life of dams by constructing reservoirs with large storage capacities relative to the volume of incoming sediment [1]. The third measure (Fig. **6c**) promotes sustainability by increasing the water-use efficiency of *HD* sediment transport.

DISCUSSION AND CONCLUSION

We asked two questions in the introduction. First, is the potential for sustainable reservoir management threatened by a threshold rate of impounded water consumption beyond which storage capacity is lost because sediment can no longer be transported through the *HD* pipeline at the rate that it enters the reservoir? Second, what are the dynamic properties of the reservoir in transition through such a threshold?

The answers to these questions depend on how the reservoir is managed. We posed a set of general management rules that broadly apply to multi-purpose public projects. First, the reservoir manager dedicates a maximum allowable consumption rate $\left(C^m\right)$ of impounded water to satisfy contractual obligations for multiple uses including hydropower production, irrigation, municipal water supplies, and so on. Second, the manager has the flexibility to adjust contractual obligations downward to provide impounded water required for restoration of lost storage capacity due to sedimentation. We accounted for this flexibility with a feedback rule that decreases impounded water allocated to meet contractual obligations as storage capacity is lost. As a result, more water remains in the reservoir to provide the potential energy for the *HD* sediment-removal pipeline. We embedded these management rules into a reservoir sedimentation model, and drew baseline parameter values from a case study of *HD* use in the Tianjiawan reservoir, China.

In answer to the first question, we found a bifurcation threshold for C^m. In terms of the scaled parameter, c^m, the bifurcation occurs when the maximum allowable consumption rate equals 48.3% of maximum reservoir storage capacity. Sustainable reservoir management is physically possible when the maximum allowable consumption rate is less than the 48.3% threshold. Two equilibria provide the necessary 'impounded-water balance' (the annual refill rate is balanced by the sum of the rates at which impounded water is consumed by contractual obligations, sediment removal requirements, and evaporation), and 'sediment balance' (reservoir storage capacity is sustained because sufficient im-

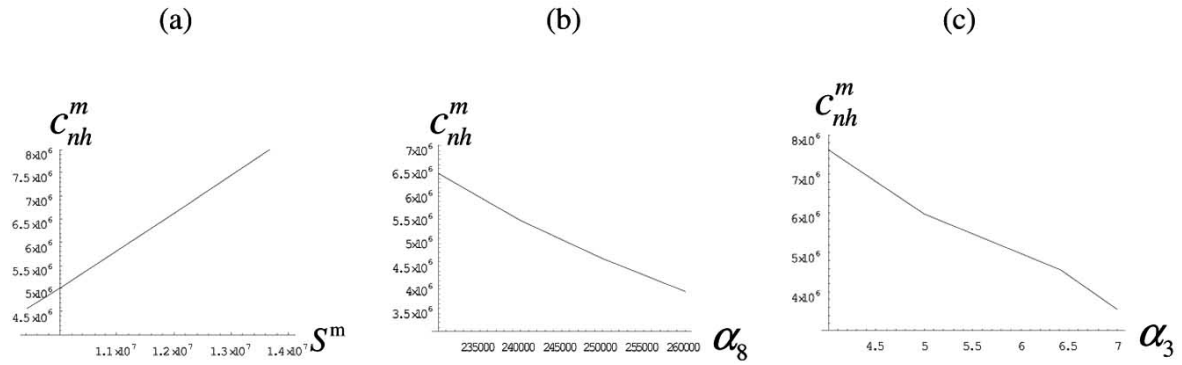

Fig. (6). Plots of c_{nh}^m against (**a**) increasing maximum storage capacity S^m; (**b**) increasing sediment entrapment rate, a_8; and (**c**) increasing proportion of water needed to transport one unit of sediment, α_3.

pounded water is allocated to provide the potential energy required for the *HD* pipeline to remove sediment at the rate it enters the reservoir). One of the equilibria is a saddle point whose convergent separatrices divide initial storage capacities into two basins of attraction. Relatively smaller initial capacities to the left of this boundary are drawn toward reservoir 'death' (i.e., a complete loss of storage capacity to sedimentation). Alternatively, relatively larger initial capacities to the right of this boundary are drawn toward a stable-node equilibrium and sustained reservoir management.

In answer to the second question, we found that the potential for sustainable reservoir management is abruptly foreclosed when the maximum allowable consumption rate exceeds the 48.3% threshold of maximum reservoir storage capacity. Volumes of impounded water and storage capacity balancing impounded-water dynamics are less than those required to balance sediment inflow and transport rates. Contractual obligations are too large in proportion to maximum storage capacity for the reservoir to furnish the potential energy required for the *HD* pipeline to remove sediment at its inflow rate. The percentage threshold can be expanded—along with the potential for sustainable reservoir management using the *HD* technology—by constructing larger reservoirs relative to the volume of incoming sediment and increasing the water-use efficiency of the *HD* pipeline.

APPENDIX

The first step in converting (4) to the generalized normal form (5) is to transform (4) to new variables that shift the nonhyperbolic equilibrium, S_{nh}^{SS}, and the scaled consumption rate generating it, c_{nh}^{SS}, to the origin: $s_1 = s - s_{nh}^{SS}$, $w_1 = w - w_{nh}^{SS}$, and $c_1^m = c^m - c_{nh}^m$:

$$\begin{aligned}\dot{w}_1 &= \left(s_1 + s_{nh}^{SS}\right) - \left(w_1 + w^{SS}\right) - \\ &\left\{\left(c_1^m + c_{nh}^m\right)\left(s_1 + s_{nh}^{SS}\right)\left(w_1 + w_{nh}^{SS}\right) / \left\{\left(w_1 + w_{nh}^{SS}\right) + \beta_1\left[1 - \left(s_1 + s_{nh}^{SS}\right)\right]\right\}\right\} \\ &- \left\{\alpha_3\beta_2\left(w_1 + w_{nh}^{SS}\right) / \left[\left(w_1 + w_{nh}^{SS}\right) + \beta_3 + \alpha_6\left(s_1 + s_{nh}^{SS}\right)\right]\right\} - \beta_4\left(w_1 + w_{nh}^{SS}\right)\end{aligned} \tag{A.1}$$

$$\dot{s}_1 = \left\{\beta_2\left(w_1 + w_{nh}^{SS}\right) / \left[\left(w_1 + w_{nh}^{SS}\right) + \beta_3 + \alpha_6\left(s_1 + s_{nh}^{SS}\right)\right]\right\} - \beta_5 \tag{A.2}$$

$$\frac{dc_1^m}{d\tau} = \dot{c}_1^m = 0 \tag{A.3}$$

where $\left(s_{nh}^{SS}, w_{nh}^{SS}, c_{nh}^m\right) = \left(0.586, 0.258, 0.483\right)$.

To compel the nonlinear portions of (A.1) and (A.2) to satisfy the normal form restrictions for (5), i.e., $Df(0,0,0) = 0 = Dg(0,0,0)$], we approximate (A.1) and (A.2) with a multivariate Taylor Series expansion:

$$\begin{pmatrix}\dot{w}_1 \\ \dot{s}_1\end{pmatrix} = \begin{pmatrix}\dot{w}_1 \\ \dot{s}_1\end{pmatrix}\Bigg|_{\left(w_1=0, s_1=0, c_1^m=0\right)} + \underbrace{\begin{pmatrix}\dfrac{\partial \dot{w}_1}{\partial w_1} & \dfrac{\partial \dot{w}_1}{\partial s_1} \\ \dfrac{\partial \dot{s}_1}{\partial w_1} & \dfrac{\partial \dot{s}_1}{\partial s_1}\end{pmatrix}\Bigg|_{\left(w_1=0, s_1=0, c_1^m=0\right)}}_{\text{Jacobian Matrix}} \begin{pmatrix}w_1 \\ s_1\end{pmatrix} + \begin{pmatrix}j\left(w_1, s_1; c_1^m\right) \\ k\left(w_1, s_1; c_1^m\right)\end{pmatrix} \tag{A.4}$$

where:

$$\begin{aligned}j\left(w_1, s_1; c_1^m\right) &= \frac{\partial \dot{w}_1}{\partial c_1^m} c_1^m + 0.5 \\ &\left(\frac{\partial^2 \dot{w}_1}{\partial w_1^2} w_1^2 + \frac{\partial^2 \dot{w}_1}{\partial s_1^2} s_1^2 + \frac{\partial^2 \dot{w}_1}{\partial (c_1^m)^2} (c_1^m)^2 + 2\frac{\partial^2 \dot{w}_1}{\partial w_1 \partial s_1} w_1 s_1\right. \\ &\left. + 2\frac{\partial^2 \dot{w}_1}{\partial w_1 \partial c_1^m} w_1 c_1^m + 2\frac{\partial^2 \dot{w}_1}{\partial s_1 \partial c_1^m} w_1 c_1^m\right)\end{aligned} \tag{A.5}$$

$$\begin{aligned}k\left(w_1, s_1; c_1^m\right) &= \frac{ds_1}{dc_1^m} c_1^m + 0.5 \\ &\left(\frac{\partial^2 \dot{s}_1}{\partial w_1^2} w_1^2 + \frac{\partial^2 \dot{s}_1}{\partial s_1^2} s_1^2 + \frac{\partial^2 \dot{s}_1}{\partial (c_1^m)^2} (c_1^m)^2 + 2\frac{\partial^2 \dot{s}_1}{\partial w_1 \partial s_1} w_1 s_1\right. \\ &\left. + 2\frac{\partial^2 \dot{s}_1}{\partial w_1 \partial c_1^m} w_1 c_1^m + 2\frac{\partial^2 \dot{s}_1}{\partial s_1 \partial c_1^m} w_1 c_1^m\right)\end{aligned} \tag{A.6}$$

Terms in (A.1) and (A.2), including the perturbation parameter, c_1^m, are viewed as nonlinear and included in

$j\left(w_1, s_1; c_1^m\right)$ and $k\left(w_1, s_1; c_1^m\right)$ in (A.5) and (A.6) [18]. Using parameter values in Table **1**, and the definitions of dimensionless parameters in Table **2**, the numerical expansion of (A.4) is:

$$\begin{bmatrix} \frac{dw_1}{d\tau} \\ \frac{ds_1}{d\tau} \end{bmatrix} = \underbrace{\begin{bmatrix} -1.74946 & 0.770295 \\ 0.0713088 & -0.031397 \end{bmatrix}}_{J} \begin{bmatrix} w_1 \\ s_1 \end{bmatrix} + \begin{bmatrix} \underbrace{-0.316918c_1^m + 0.5\begin{pmatrix} 2.22347w_1^2 - 1.43377s_1^2 - 0.216369s_1w_1 - \\ 1.12812c_1^m w_1 - 1.78497c_1^m s_1 \end{pmatrix}}_{j\left(w_1, s_1; c_1^m\right)} \\ \underbrace{0.5\left(-0.168901w_1^2 + 0.0743665s_1^2 - 0.0945347s_1w_1\right)}_{k\left(w_1, s_1; c_1^m\right)} \end{bmatrix}$$

$$\dot{c}_1^m = 0 \qquad \text{(A.7)}$$

The last step in converting (4) to normal form (5) is to introduce new variables $\left(s_2, w_2\right)$ that diagonalize the Jacobian matrix in (A.4): $\begin{pmatrix} w_1 \\ s_1 \end{pmatrix} = \underbrace{\begin{pmatrix} \text{-0.99917} & \text{-0.402972} \\ 0.0407266 & \text{-0.915212} \end{pmatrix}}_{P} \begin{pmatrix} w_2 \\ s_2 \end{pmatrix}$, where the columns of P are the eigenvectors of the Jacobian matrix. The resulting normal form is:

$$\begin{pmatrix} \dot{w}_2 \\ \dot{s}_2 \end{pmatrix} = \underbrace{\begin{pmatrix} -1.781 & 0 \\ 0 & 0 \end{pmatrix}}_{P^{-1}JP} \begin{pmatrix} w_2 \\ s_2 \end{pmatrix} + \underbrace{\begin{pmatrix} \text{-0.983185} & 0.4329 \\ \text{-0.0437514} & \text{-1.07338} \end{pmatrix}}_{P^{-1}} \begin{pmatrix} j\left(w_1(w_2, s_2), s_1(w_2, s_2); c_1^m\right) \\ k\left(w_1(w_2, s_2), s_1(w_2, s_2); c_1^m\right) \end{pmatrix}$$

$$= \begin{pmatrix} -1.781 & 0 \\ 0 & 0 \end{pmatrix} \begin{pmatrix} w_2 \\ s_2 \end{pmatrix} + \begin{pmatrix} 0.452109s_2^2 - 1.02656c_m^1 s_2 + 0.311589c_1^m - \\ 1.13003w_2^2 - 0.886238s_2w_2 - 0.518379c_1^m w_2 \\ \\ 0.02011962s_2^2 - 0.0456814c_m^1 s_2 + 0.0138656c_1^m + \\ 0.0396664w_2^2 + 0.0842781s_2w_2 - 0.0230677c_1^m w_2 \end{pmatrix} \qquad \text{(A.8)}$$

$$\dot{c}_1^m = 0 \qquad \text{(A.9)}$$

where the eigenvalues of the Jacobian matrix (-1.781, 0) are along the diagonal of the 2×2 matrix in (A.8).

ACKNOWLEDGEMENT

Partial funding for this work was provided by NSF EF-0531870.

REFERENCES

[1] Morris G, Fan J. Reservoir sedimentation handbook, McGraw-Hill: New York 1998.

[2] White R. Evacuation of sediments from reservoirs. Thomas Telford: London 2001.

[3] Mahmood K. Reservoir Sedimentation: Impact, Extent, Mitigation. World Bank Technical Report No. 71: Washington, DC 1987.

[4] Batuca D, Jordaan J. Silting and desilting of reservoirs. Taylor and Francis: London 2000.

[5] Palmieri A, Shaw F, Dinar A. Economics of reservoir sedimentation and sustainable management of dams. J Environ Manag 2001; 61: 149-63.

[6] Matilija Dam Ecosystem Restoration Project-Homepage. http://www.matilijadam.org/ [access: October 9, 2009].

[7] Foundation for Water Research. World Water Storage in Man-Made Reservoirs. FR/R0012: Marlow, UK 2005.

[8] Coker E, Hotchkiss R, Johnson D. Conversion of a missouri river dam and reservoir to a sustainable system. University of South Dakota, Department of Chemistry Working Paper 2007.

[9] Palmieri A, Shaw F, Annandale G, Dinar A. Reservoir conservation: The RESCON Approach. The World Bank: Washington DC, 2003.

[10] Kawashima S, Johndrow T, Annandale G, Shaw F. Reservoir conservation: RESCON Model and User Manual. The World Bank: Washington, DC 2003.

[11] Huffaker R, Hotchkiss R. Economic dynamics of reservoir sedimentation management: optimal control with singularly perturbed equations of motion. J Econ Dyn Control 2006; 30: 2553-75.

[12] Hotchkiss R, Huang X. Hydrosuction Sediment-Removal Systems (HSRS): Principles and field test. J Hydraul Eng 1995; 121: 479-89.

[13] Department of the Army. Columbia River Pump Station Permit 1995.

[14] Liu J, Liu B, Ashida K. Reservoir sedimentation management in asia. In: Proceedings of the international conference on hydroscience and engineering (ICHE); Warsaw 2002.

[15] Linsley R, Franzini J, Freyberg D, Tchobanoglous G. Water resources engineering, 4th ed. McGraw-Hill: New York 1992.

[16] ReVelle C. Optimizing reservoir resources. Wiley: New York 1999.

[17] Glendinning P. Stability, instability and chaos: An introduction to the theory of nonlinear differential equations. Cambridge University Press: New York 1995.

[18] Wiggins S. Introduction to Applied Nonlinear Dynamic Systems and Chaos 2d, Springer: New York 2000.

Received: October 13, 2009 Revised: August 06, 2010 Accepted: August 16, 2010